

MIZMAS: Modeling the Evolution of Ice Thickness and Floe Size Distributions in the Marginal Ice Zone of the Chukchi and Beaufort Seas

Jinlun Zhang

Applied Physics Laboratory, University of Washington
1013 NE 40th St
Seattle, WA 98105

phone: (206) 543-5569 fax: (206) 616-3142 email: zhang@apl.washington.edu

Axel Schweiger

Applied Physics Laboratory, University of Washington
1013 NE 40th St
Seattle, WA 98105

phone: (206) 543-1312 fax: (206) 616-3142 email: axel@apl.washington.edu

Michael Steele

Applied Physics Laboratory, University of Washington
1013 NE 40th St
Seattle, WA 98105

phone: (206) 543-6586 fax: (206) 616-3142 email: mas@apl.washington.edu

Grant Number: N00014-12-1-0112

LONG-TERM GOALS

Our long-term goal is to develop a robust, high-resolution coupled sea ice–ocean modeling and assimilation system that is capable of accurately predicting sea ice conditions in the marginal ice zone (MIZ) of the Chukchi and Beaufort seas (CBS) on seasonal time scales. Our primary interest is the ability to realistically simulate the evolution of the multicategory ice thickness and floe size distributions (ITD, FSD) jointly in the CBS MIZ. Particularly, we would like to improve model physics to represent changes in FSD due to ice advection, thermodynamic growth or decay, lateral melting, ridging and rafting, and wave-induced fragmentation through theoretical development and numerical implementation.

OBJECTIVES

Our main scientific objectives are to:

- (1) Examine the historical evolution of the CBS MIZ ice–ocean system and its ITD and FSD from 1978 to the present to quantify and understand the large-scale changes that have occurred in the system.
- (2) Identify key linkages and interactions among the atmosphere, sea ice, and ocean, to enhance our understanding of mechanisms affecting the CBS MIZ dynamic and thermodynamic processes.

- (3) Explore the predictability of the seasonal evolution of the MIZ and the summer location of the ice edge in the CBS through seasonal ensemble forecast.
- (4) Explore the impacts of future anthropogenic global climate change (including a summer arctic ice-free regime) on the CBS MIZ processes through downscaling future projection simulations.

APPROACH

To address the scientific objectives, we plan to develop, implement, and validate a new coupled ice–ocean **Marginal Ice Zone Modeling and Assimilation System (MIZMAS)** that will enhance the representation of the unique MIZ processes by incorporating a FSD and corresponding model improvements. A successful incorporation of a FSD will allow MIZMAS to simulate the evolution of both ITD and FSD at the same time. The development of MIZMAS will be based on systematic model parameterization, calibration, and validation, and data assimilation, taking advantage of the integrated observational and modeling efforts planned by the ONR MIZ research initiative. Meanwhile, we also use the **Pan-arctic Ice/Ocean Modeling and Assimilation System (PIOMAS)**, a variant of MIZMAS, to study changes in the Arctic sea ice and ocean system. With a coarser model resolution than MIZMAS, PIOMAS is more computationally efficient in process studies. Jinlun Zhang, Axel Schweiger, Mike Steele at the University of Washington are investigators of this project. Harry Stern at UW also helped in analyzing satellite images of sea ice floes and deriving FSD. In addition, an undergraduate student at UW, Margaret Stark, continued to work on processing and analyzing satellite images of sea ice this year.

WORK COMPLETED

To enhance our understanding of MIZ processes, the observation team of the ONR MIZ program deployed five clusters of instruments of various platforms in the Beaufort Sea in March and August 2014. To support the planning of the field work, we developed an ensemble seasonal forecast system in 2013 for predicting Arctic sea ice weeks to months in advance using MIZMAS that has high-resolution coverage for the CBS. The ensemble consists of seven members each of which uses a set of NCEP/NCAR atmospheric forcing fields from one of the recent seven years. These recent seven years of the reanalysis atmospheric forcing fields are used to represent the climate variability expected for 2014. If the 2014 climate is close to any of the past seven years, it would be captured by the prediction. Each ensemble prediction starts with the same initial ice–ocean conditions. To obtain the “best possible” initial ice-ocean conditions for the forecasts, a hindcast is conducted, which assimilates satellite ice concentration and sea surface temperature data (see Zhang et al., 2008). On the first day of each month from January to July, 2014, we conducted hindcast and seasonal forecast of sea ice thickness all the way to October 2014 for the Beaufort Sea region (Figure 1).

To support the ONR MIZ field work after the clusters were deployed in March, we developed a numerical framework for 48 hour forecast of sea ice thickness and drift in and around the Beaufort Sea MIZ using MIZMAS. The short-term sea ice forecast system was forced by the forecast atmospheric data from the NCEP (National Center for Environmental Prediction) Climate Forecast System version 2 (CFSv2). The CFSv2 forecast ranges from hours to months and the 6-hourly forecast atmospheric data are widely accessible in real time, thus useful for forcing our sea ice forecast over a range of time scales. However, for the ONR MIZ field work, the sea ice forecast system was used to predict ice thickness in the Beaufort Sea MIZ 48 hours in advance, focusing on the areas around the five clusters. It has also been used to predict the movement of these clusters (Figure 2). We did the forecast almost

every work day from Jul 21 onward, when the instruments were taking measurements in the Beaufort Sea.

We continued to work on the incorporation of FSD into MIZMAS. We improved the FSD theory by refining the formulation of floe size redistribution due to ice ridging processes. We tested the numerical implementation of the FSD conservation equation. We also tested model sensitivity to different partitions of floe size categories for calculating FSD. While testing the FSD theory, we have been preparing a manuscript to document all the development, for possible publication in the near future.

We have been developing procedures for extracting FSD from two sets of satellite images: NASA/MODIS (pixel size 250 meters) and USGS/Global Fiducials Library (GFL) (pixel size 1 meter). We seek to establish a relationship between the FSD at the large scale and the small scale, enabling us to parameterize the important but difficult-to-observe small-scale FSD in terms of the large-scale FSD. Landsat optical images at 15m resolution are used as well. Our project focuses on developing a database of temporally and spatially varying FSD in the Beaufort sea over several seasons that will be suitable for model initialization and validation. In addition to our analysis based on optical sensors, we are collaborating with others (e.g. Phil Huang) who are focusing on SAR-derived FSD to complement the approaches and integrate the results.

We investigated forcing mechanisms for seasonal ice loss in the Beaufort Sea. We explored the possibility of predicting the seasonal ice retreat there months in advance. We also found that the date when sea ice concentration begins to decline from its winter maximum is becoming more synchronous across the Beaufort Sea, relative to past years when this date was much earlier in the east relative to the west. Results from this investigation have been submitted to *J. Geophysical Research* (Steele et al., 2014).

We collaborated with Dr. T. Martin at University of Washington to study seasonal variability and long-term trend of Arctic Ocean surface stress over the period of 1979–2012, which are closely linked to changes in sea ice. Results from this collaboration have been published in *J. Geophysical Research* (Martin et al., 2014).

We collaborated with R. Lindsay at University of Washington to evaluate seven different atmospheric reanalysis products in the Arctic. We examined how these reanalysis products affect modeled Arctic sea ice volume variability and trends on a decadal time scale when they are used to drive model simulations. Results from this collaboration have been published in *J. Climate* (Lindsay et al., 2014).

RESULTS

Modeling:

In our seasonal forecast effort, we focus on the prediction of ice edge locations in the CBS. This year, we found that, with the prediction starting on June 1, MIZMAS predicted ice edge locations are generally not too far away from satellite (SSM/I) observed ice edge locations in much of the CBS on August 18, 2014 when four ONR MIZ clusters of instruments were mostly in the Beaufort Sea MIZ (Figure 1). This is encouraging considering the challenge in accurate seasonal prediction of ice edge locations.

In our short-term (48 hour) forecast effort, we focus on the prediction of both ice thickness and ice drift represented by the five ONR MIZ clusters (Figure 2). To examine the accuracy of MIZMAS simulated ice thickness in 2014, we compared MIZMAS ice thickness with the quick-look ice thickness data from the NASA mission Operation IceBridge (data courtesy of Nathan Kurtz). The IceBridge data were collected between 12 March and 3 April across broad regions of the Beaufort and Chukchi seas and the Canadian Basin. The point data were clustered into 50-km averages by R. Lindsay and used for a model-observation comparison. There are 197 clustered data points for the CBS that are compared with corresponding MIZMAS results (Figure 3a). The locations of these data points and the model-observation differences are shown in Figure 3b. MIZMAS is in good agreement with IceBridge observations in the CBS, with mean model bias of 0.02 m. The model-observation correlation is 0.84, indicating that MIZMAS captures about 70% of the variance of the 2014 IceBridge data.

Remote Sensing:

MODIS images are downloaded automatically from the NASA Global Imagery Browse Service via the Web Map Service interface. Cloud-free regions in the images are delineated manually based on visible and near-infrared bands 3-6-7. We have processed 87 images (129 cloud-free regions) for the period May–October, 2013, in a Beaufort Sea region (blue outline, Figure 4a). The median size of the cloud-free regions is about 80,000 km². A low-pass filter (Gaussian) with length scale 25 km is applied to a cloud-free region (red in Figure 4a and full view in Figure 4b), and the smoothed image is subtracted from the original image. Positive differences are assigned a value 1 (ice); negative differences are assigned a value 0 (water). This creates a binary image (Figure 5a). After that, a morphological *erosion* operation is applied to the binary image in order to separate ice floes that are touching. Floes in the resulting eroded image are labeled using a recursive algorithm that identifies groups of connected pixels (Figure 5b). Floes are then “re-grown” outward using a variation of the morphological *dilation* operation in which only those pixels that were originally assigned as ice are allowed to re-grow. Properties of each floe are then easily calculated, such as area, perimeter, and caliper diameter. This allows us to obtain the number density, which is defined as the number of floes of a given size within the cloud-free region divided by the area of the region. The number density is one way to express the FSD.

Using the method described above, we have been able to derive satellite FSD. Figure 6 shows the number density of floes as a function of their mean caliper diameter for three different locations in the Beaufort Sea on three different days in May, 2013. The FSD follows a power-law distribution with slope (in log-log space) -2.0 .

Changes in Sea Ice in the Beaufort Sea:

We studied sea ice changes in the Beaufort Sea over the past decades. We found that ice opening is generally late in the western Beaufort owing to advection of old, thick ice from the northeast, but this is trending toward earlier dates as thick ice has recently thinned. Meanwhile, opening is early in the eastern Beaufort owing to easterly winds in spring, and this has not changed over time. The result is that opening is becoming more synchronous across the Beaufort Sea, i.e., seasonal ice loss is becoming more zonally uniform (Figure 7). This also holds for the Date of ice Retreat (DOR, defined as the final day when concentration falls below 15%) although with less statistical significance relative to the Date of ice Opening (DOO, defined as the final day of the spring/summer when ice concentration falls below 80%) (Steele et al., 2014).

Interpretation of FSD Curves:

In the literature on the sea-ice floe size distribution, some researchers plot the *number density* (ND) vs. floe size x , and some plot the *reverse cumulative number density* (RCND) vs. floe size. If the ND follows a power-law distribution over a finite range of floe sizes, then the RCND is of the form: (power law) $- h$ where h is a constant. This gives the RCND a concave-down shape in log-log space. At least one research group (Toyota et al., 2011) has observed this concave-down shape and interpreted it as two physical regimes, each following a power-law distribution with different slopes. We believe that this interpretation is incorrect. Figure 8 is taken from Toyota et al. (2011), with annotation added by us: we have selected three points along the blue curve (Oct 18) and added a constant value of $h=80$ to them. This raises the three points up to the black line that matches the slope of the blue curve for floe sizes < 20 meters. Toyota et al. claim that there is a break-point in the slope of the distribution at floe sizes between 20 and 40 meters. But our analysis of this figure shows that the data are consistent with a single power-law ND over the range $2 \text{ meters} < x < 100 \text{ meters}$, and that the concave-down shape of the RCND is simply due to the finite domain. It is not necessary to postulate different physical processes affecting large and small floes. This points to the need for careful interpretation of ND and RCND representations of the floe size distribution.

IMPACT/APPLICATIONS

The objectives of this project address directly some of the key questions raised in the ONR MIZ research initiative: *Emerging Dynamics of the Marginal Ice Zone*. These questions are explored by modeling, analyzing, and understanding the large-scale changes that have occurred in the CBS MIZ, and by assessing the possible changes that lie ahead. Aiming to improve our understanding of the CBS MIZ processes, interactions, and feedbacks, this ONR MIZ research contributes to the inter-agency Study of Environmental Arctic Change (SEARCH). Aiming to enhance model physics, this research addresses the U.S. Navy's needs to improve the predictability of sea ice in the region. A successful development of MIZMAS will mark a new sea ice model that is able to explicitly simulate the evolution of multicategory ice thickness and floe size distributions simultaneously. The theoretical and numerical work on FSD will provide a foundation to improve significantly the representation of key MIZ processes. This will be a significant step forward towards developing the next generation of sea ice models for use in operational forecast and climate predictions.

RELATED PROJECTS

Supported by NASA and in collaboration with Drs. Carin Ashjian, Robert Campbell, Victoria Hill, Yvette Spitz, Zhang and Steele are investigating planktonic ecosystem response to changing sea ice and upper ocean physics in the CBS. We are modeling the integrated system of sea ice, ocean, and marine ecosystem in the CBS (http://psc.apl.washington.edu/zhang/Chukchi_Beaufort/model.html).

REFERENCES

- Toyota, T., C. Haas, and T. Tamura, Size distribution and shape properties of relatively small sea-ice floes in the Antarctic marginal ice zone in late winter, *Deep-Sea Research II*, 58, 1182–1193, doi:10.1016/j.dsr2.2010.10.034, 2011.
- Zhang, J., M. Steele, R.W. Lindsay, A. Schweiger, and J. Morison, Ensemble one-year predictions of arctic sea ice for the spring and summer of 2008. *Geophys. Res. Lett.*, 35, L08502, doi:10.1029/2008GL033244, 2008.

PUBLICATIONS

- Laxon, W.S., K. A. Giles, A. L. Ridout, D. J. Wingham, R. W., R. Cullen, R. Kwok, A. Schweiger, J. Zhang, C. Haas, S. Hendricks, R. Krishfield, N. Kurtz, S. Farrell, M. Davidson, CryoSat-2 estimates of Arctic sea ice thickness and volume, *Geophys. Res. Lett.*, doi:10.1002/grl.5019, 2013 [published, refereed].
- Lindsay, R., C. Haas, S. Hendricks, P. Hunkeler, N. Kurtz, J. Paden, B. Panzer, J. Sonntag, J. Yungel, and J. Zhang, Seasonal forecasts of arctic sea ice initialized with observations of ice thickness, *Geophys. Res. Lett.*, 39, L21502, doi:10.1029/2010GL053576, 2012 [published, refereed].
- Lindsay, R., M. Wensnahan, A. Schweiger, and J. Zhang, Evaluation of seven different atmospheric reanalysis products in the Arctic, *J. Climate*, 27, 2588-2606, doi: <http://dx.doi.org/10.1175/JCLI-D-13-00014.s1>, 2014 [published, refereed].
- Martin, T., M. Steele, and J. Zhang, Seasonality and long-term trend of Arctic Ocean surface stress in a model, *J. Geophys. Res.*, 119, 1723-1738, doi:10.1002/2013JC009425, 2014 [published, refereed].
- Miller, R. L., G. A. Schmidt, L. S. Nazarenko, N. Tausnev, R. Ruedy, M. Kelley, K. K. Lo, I. Aleinov, M. Bauer, S. Bauer, R. Bleck, V. Canuto, Y. Cheng, T. L. Clune, A. DelGenio, G. Faluvegi, J. E. Hansen, R. J. Healy, N. Y. Kiang, D. Koch, A. A. Lacis, A. N. LeGrande, J. Lerner, J. Marshall, S. Menon, V. Oinas, J. Perlwitz, M. J. Puma, D. Rind, A. Romanou, G. L. Russell, M. Sato, D. T. Shindell, S. Sun, K. Tsigaridis, N. Unger, A. Voulgarakis, M.-S. Yao, and J. Zhang, CMIP5 historical simulations (1850-2012) with GISS ModelE2. *J. Advances in Modeling Earth Systems*, 6, no. 2, 441-477, doi:10.1002/2013MS000266, 2014 [published, refereed].
- Nazarenko, L.S., G. A. Schmidt, R.L. Miller, N. Tausnev, M. Kelley, R. Ruedy, G.L. Russell, I. Aleinov, M. Bauer, S. Bauer, R. Bleck, V. Canuto, Y. Cheng, T. L. Clune, A. DelGenio, G. Faluvegi, J. E. Hansen, R. J. Healy, N. Y. Kiang, D. Koch, A. A. Lacis, A. N. LeGrande, J. Lerner, K. K. Lo, S. Menon, V. Oinas, J. Perlwitz, M. J. Puma, D. Rind, A. Romanou, M. Sato, D. T. Shindell, S. Sun, K. Tsigaridis, N. Unger, A. Voulgarakis, M.-S. Yao, and J. Zhang, Future Climate Change under RCP Emission Scenarios with the GISS ModelE2, *J. Advances in Modeling Earth Systems*, 2013 [submitted, refereed].
- Peralta-Ferriz, C., J.H. Morrison, J.M. Wallace, J.A. Bonin, and J. Zhang, Arctic Ocean circulation patterns revealed by GRACE, *J. Climate*, 27, 1445-1468, doi:10.1175/JCLI-D-13-00013.1, 2014 [published, refereed].
- Schmidt, G. A., M. Kelley, L. Nazarenko, R. Ruedy, G. L. Russell, I. Aleinov, M. Bauer, S. Bauer, M. K. Bhat, R. Bleck, V. Canuto, Y. Chen, Y. Cheng, T. L. Clune, A. DelGenio, R. de Fainchtein, G. Faluvegi, J. E. Hansen, R. J. Healy, N. Y. Kiang, D. Koch, A. A. Lacis, A. N. LeGrande, J. Lerner, K. K. Lo, J. Marshall, E. E. Mathews, S. Menon, R. L. Miller, V. Oinas, A. Olos, J. Perlwitz, M. J. Puma, W. M. Putman, D. Rind, A. Romanou, M. Sato, D. T. Shindell, S. Sun, R. Syed, N. Tausnev, K. Tsigaridis, N. Unger, A. Voulgarakis, M.-S. Yao, and J. Zhang, Configuration and assessment of the GISS ModelE2 contributions to the CMIP5 archive. *J. Advances in Modeling Earth Systems*, 6, no. 2, 141-184, doi:10.1002/2013MS000265, 2014 [published, refereed].
- Steele, M., S. Dickinson, and J. Zhang, Seasonal ice loss in the Beaufort Sea: Toward synchronicity and prediction, *J. Geophys. Res.*, submitted, 2014 [submitted, refereed].

Zhang, J., R. Lindsay, A. Schweiger, and I. Rigor, Recent changes in the dynamic properties of declining Arctic sea ice: A model study, *Geophys. Res. Lett.*, *39*, L20503, doi:10.1029/2012GL053545, 2012 [published, refereed].

Zhang, J., R. Lindsay, A. Schweiger, and M. Steele, The impact of an intense summer cyclone on 2012 Arctic sea ice retreat, *Geophys. Res. Lett.*, *40*, doi:10.1002/grl.50190, 2013 [published, refereed].

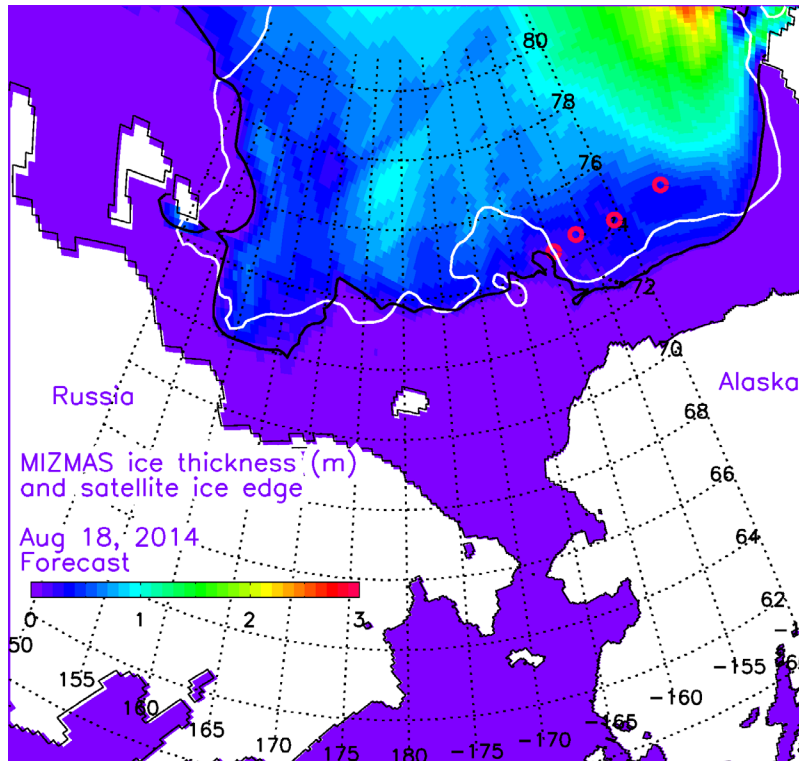


Figure 1. MIZMAS seasonal prediction of sea ice thickness (colors) and edge (black line) and satellite passive microwave observation of ice edge (white line) in the Pacific sector of the Arctic Ocean on August 18, 2014 when four ONR MIZ clusters of instruments were in the CBS MIZ (red circles). Ice edge is defined as the contour of 0.15 ice concentration. The prediction started on June 1, 2014, and so the prediction range was 2 months and 18 days. The seasonal prediction was meant to give a rough idea of ice thickness distribution and ice edge location months ahead in the areas where four ONR MIZ clusters of instruments were deployed in March and one in August.

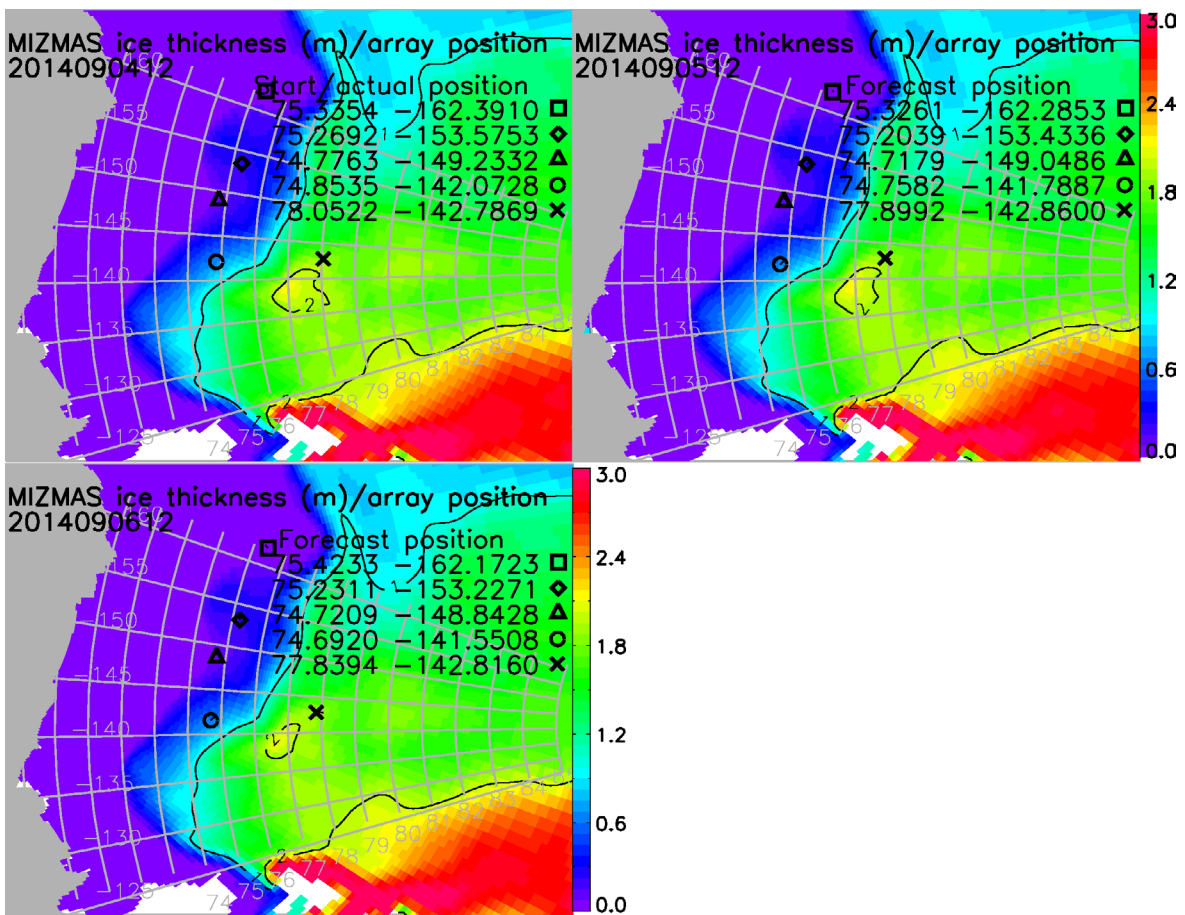


Figure 2. MIZMAS short-term forecast of sea ice thickness and the drift of five clusters of instruments (marked by square, diamond, triangle, circle, and cross) deployed in the Beaufort Sea in 2014 by the ONR MIZ program. This figure shows initial MIZMAS ice thickness and actual cluster positions at the 12th hour on September 4, 2014 (upper left), and one (upper right) and two (lower) day prediction of ice thickness and cluster positions.

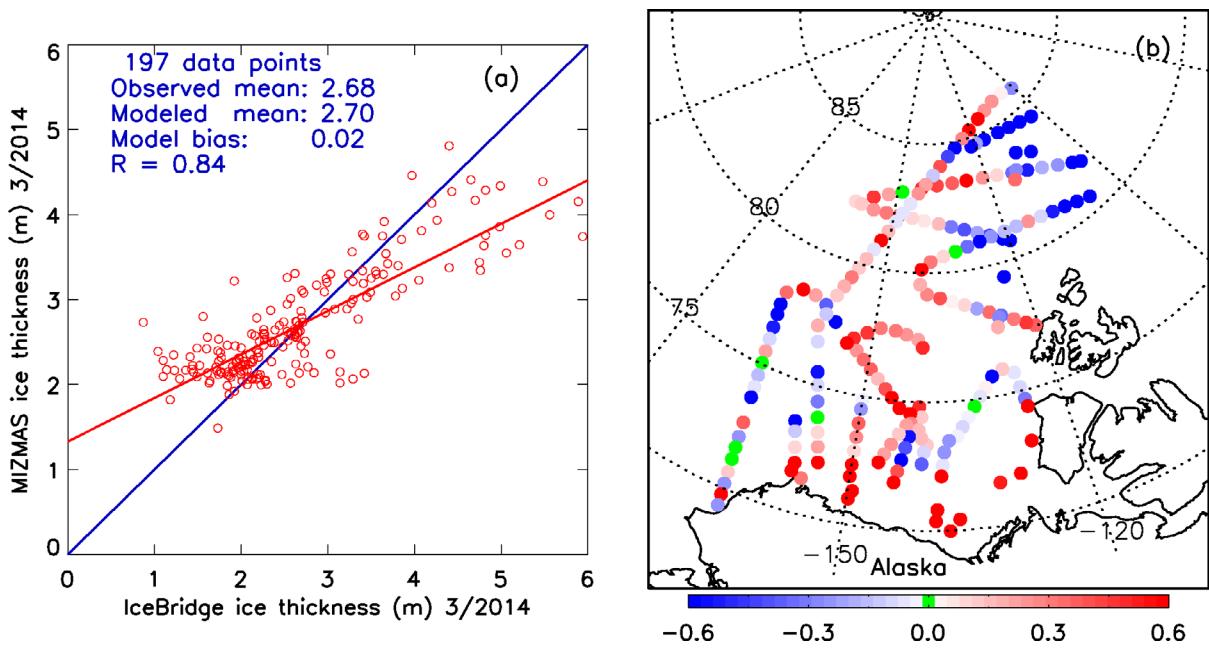


Figure 3. (a) A comparison of available sea ice thickness (m) data from the NASA IceBridge program collected during March, 2014 in the Chukchi and Beaufort seas. The blue line indicates equality and the red line represents the best fit to the observations. The IceBridge point data were clustered into 50-km averages by R. Lindsay and compared with corresponding model results. The number of total clustered observation points, model and observation mean values, model bias (mean model-observation difference), and model-observation correlation (R) are listed. **(b)** Point-by-point ice thickness differences (m) between model results and observations at the locations of the observations.

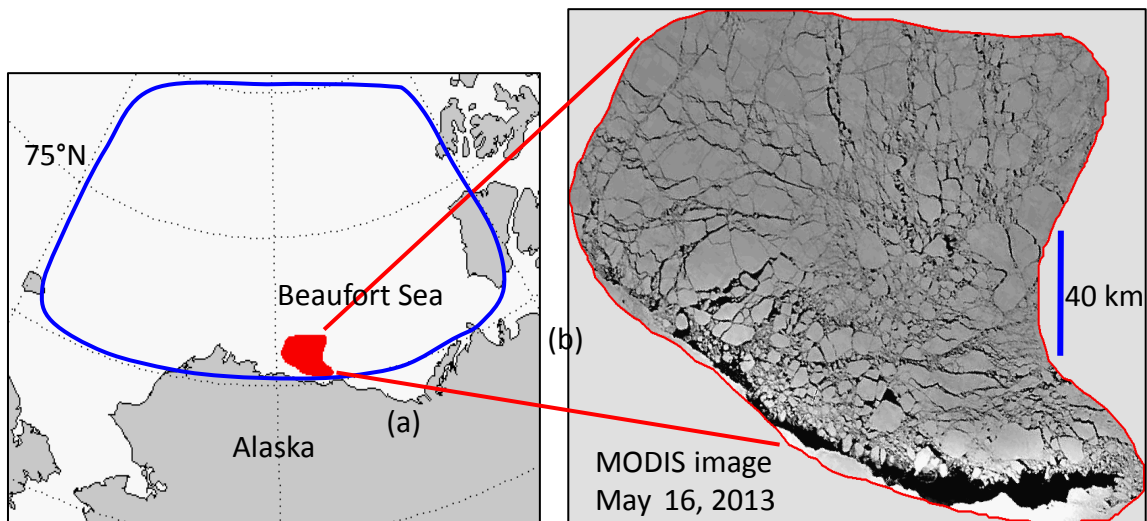


Figure 4. (a) Blue outline indicates a region in the Beaufort Sea where 87 MODIS images from May to October, 2013 were analyzed; MODIS image in a cloud-free region (in red) on May 16, 2013 is used to test the method to derive FSD. **(b)** A full MODIS image for the cloud-free region in red on that day.

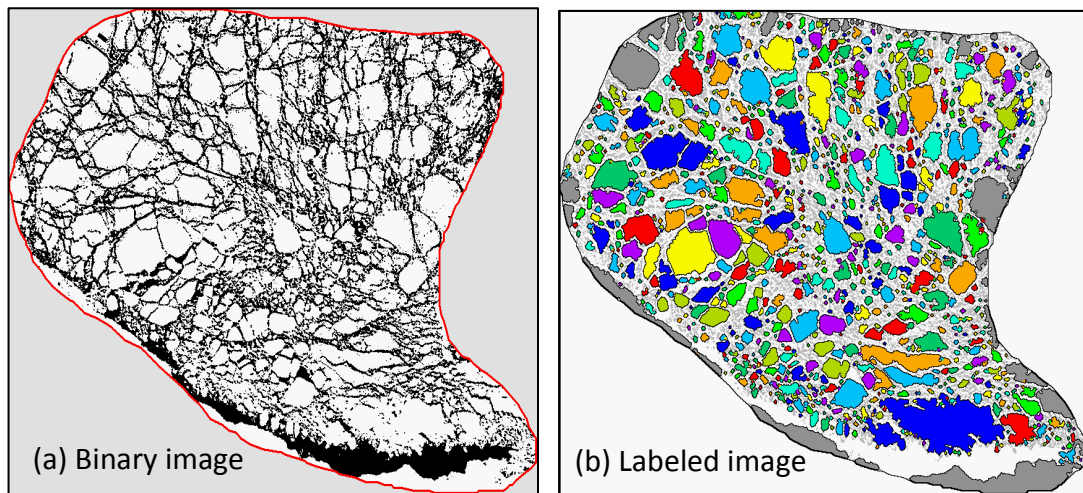


Figure 5. (a) A binary image created by applying a low-pass filter (Gaussian) with length scale 25 km to a cloud-free region shown in Figure 4. (b) A labeled image after applying the morphological erosion operation in order to obtain the properties of each, such as area, perimeter, and caliper diameter.

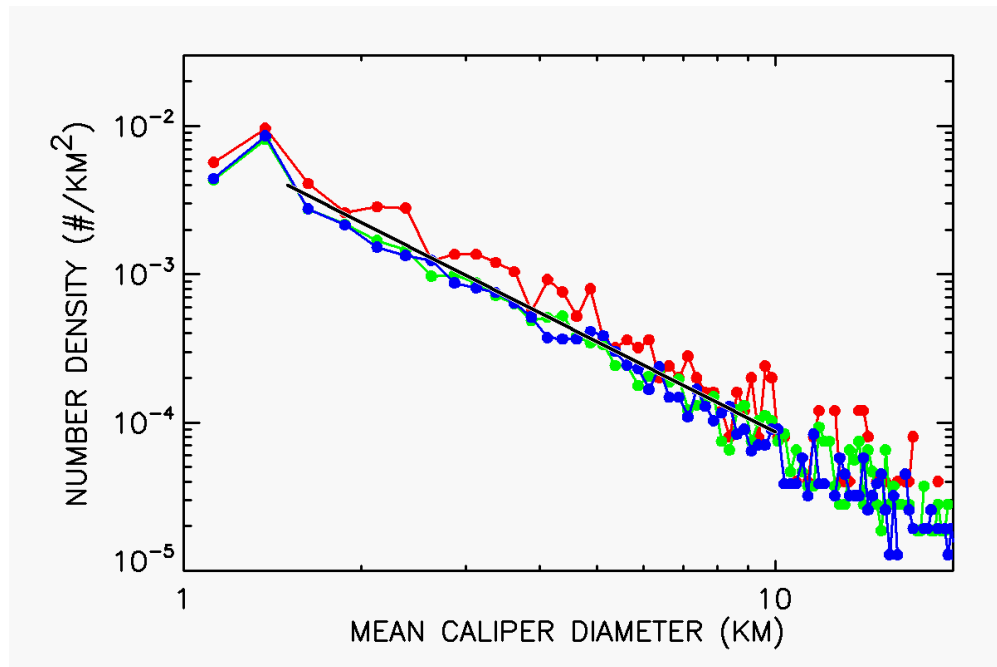


Figure 6. Number density of floes as a function of their mean caliper diameter for three different locations in the Beaufort Sea on May 16, 17, and 18, 2013.

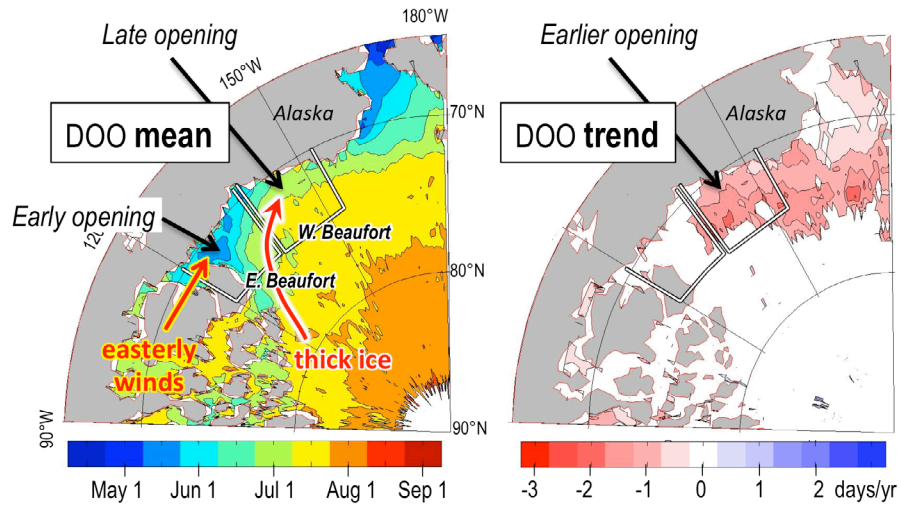


Figure 7. Date of ice Opening (DOO), defined as the final day of the spring/summer when ice concentration falls below 80%, with respect to the long-term mean over 1979–2012 (left panel) and the 95% significant linear trend (right panel), from Steele et al. (2014).

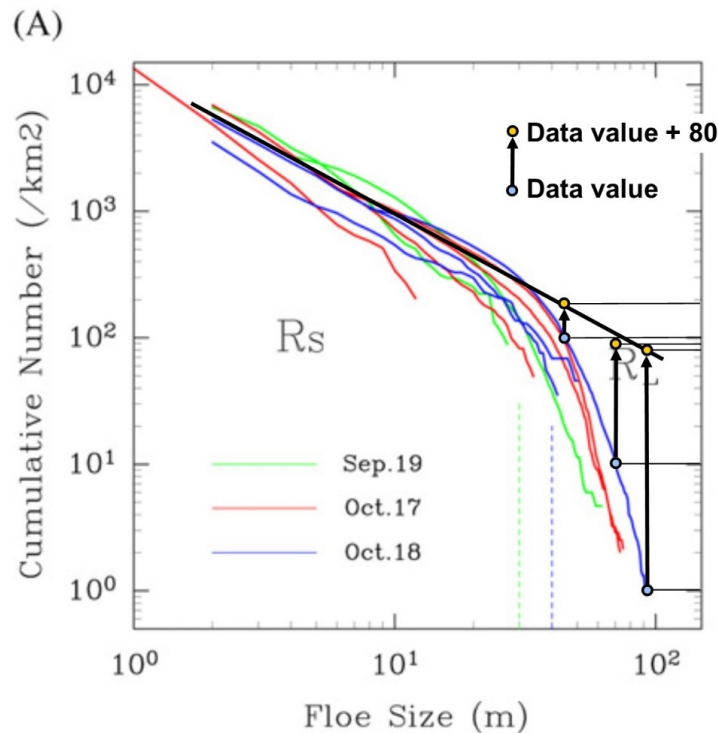


Figure 8. Taken from Toyota et al. (2011), with annotation added by us: three selected points on the blue curve of Oct 18 (blue dots); the new values after adding 80 (yellow dots); and the sloping black line, showing that the slope for floe sizes < 20 meters is consistent with the slope for floe sizes > 40 meters after accounting for the effect of the finite domain.